

Multiple-scattering Green-function method for electronic-structure calculations of surfaces and coherent interfaces

A. Gonis

University of California, Division of Chemistry and Materials Science, L-280, Lawrence Livermore National Laboratory, Livermore, California 94550

X.-G. Zhang

Center for Advanced Materials, Materials and Chemical Sciences Division, Lawrence Berkeley Laboratory, Berkeley, California 94720

J. M. MacLaren

Theoretical Division, Los Alamos National Laboratory, Los Alamos, New Mexico 87545

S. Crampin

The Blackett Laboratory, Imperial College, London SW7 ZBZ, United Kingdom

(Received 2 January 1990)

We present a formally exact solution of the multiple-scattering-theory (MST) equations for the case of semi-infinite and coherent doubly semi-infinite materials. For the case of semi-infinite materials (surfaces), we also present an alternative approach based upon the embedded-cluster method, which can be numerically as accurate as the exact method but is computationally easier to implement. The methods presented here satisfy the correct boundary conditions associated with semi-infinite materials and thus constitute a proper generalization of the Green-function formalism as applied to bulk systems, to the treatment of surfaces and interfaces. Specifically, the lack of translational invariance in directions perpendicular to the surface or interface is handled through the solution of a self-consistent equation for the scattering matrix, describing exactly the interaction of any chosen plane near the surface or interface with the rest of the material. The formalism is free of the introduction of extraneous conditions such as the artificial truncation of the free-particle propagator or the range of electron hopping elements, or the use of a complex potential. Furthermore, being based on a first-principles, MST Green-function method, the formalism is applicable to the treatment of a large number of physically important problems such as surface and/or interface regions formed by pure materials or concentrated alloys, the study of impurities of diverse kinds near such a region, and many others. Results for one-dimensional model systems as well as realistic three-dimensional materials are presented. The advantages, convergence properties, and restrictions of the formalisms are discussed and further work, currently in progress, is commented upon.

I. INTRODUCTION

The proper treatment of the electronic structure near extended defects such as surface and interface regions is an indispensable requirement in the study of many technologically important properties of materials. Chemisorption, catalysis, resistance to corrosion, embrittlement, and semiconductor and device physics are only a few of the fields of interest in which the specific properties of surfaces and interfaces, grain boundaries in particular, figure in a significant way. Consequently a great number¹⁻⁶⁴ of attempts have been made in devising methods appropriate to the study of electrons in semi-infinite solids.

These attempts can be broadly classified according to the form of the Hamiltonian chosen and the approach followed in treating the lack of translational invariance in directions perpendicular to the surface or the interface. Many studies¹⁻³³ are based on a tight-binding (TB) or more generally on a linear combination of atomic orbitals or a linear combination of muffin-tin orbitals description

of the Hamiltonian. The finite range of the electron transfer-matrix elements (hopping terms) within a TB framework allows an approximate but computationally efficient and transparent treatment of the electronic structure of surfaces and interfaces within a number of different techniques. Thus, Green-function,¹⁻⁵ transfer-matrix,⁶ and continued-fraction methods⁷⁻¹⁴ have been used.

The slab approach has been used¹⁵⁻²⁵ extensively in surface calculations, with the thickness of the slab being taken large enough to minimize interference effects between the two "free" surfaces. The supercell approach has primarily been adopted in studies of interfaces. More accurate treatments of surface electronic structure than those afforded by a TB formalism can in principle be obtained through the use of pseudopotential theory³⁴⁻⁴⁰ and of *ab initio* methods⁴¹⁻⁵² based on realistic potentials of the muffin-tin (MT) or more general forms. Again a variety of techniques such as wave-function matching,³⁷⁻⁴⁰ Green-function matching,⁴¹⁻⁴⁹ and variational methods⁵⁰⁻⁵² can be employed to calculate quantities of

physical interest such as reflectivities in low-energy electron diffraction (LEED) experiments. A quite precise treatment of the surface or interface charge distribution, which has been found to be very accurate in the case of metallic systems is provided by the full potential linearized augmented plane-wave method.^{53,54} However, this method can only be employed in the presence of full translational invariance and thus can only be used in conjunction with the slab approximation to the semi-infinite solid; hence, it appears to be incapable of treating properly problems of an embedding type, e.g., dilute impurities, substitutional or interstitial, near surfaces or interfaces, or in bulk systems.

Perhaps the best known and most commonly used method for the theoretical study of surface electronic structure and particularly the analysis of LEED spectra is the layer Korringa-Kohn-Rostoker approach⁵⁵⁻⁶⁰ (LKRR), in connection with the technique of layer doubling. This method is based on the theory of multiple scattering of electrons in a field of MT potentials, but the extension to potentials of a more general shape appears to be possible,^{61,62} and is currently under rather intensive study. Multiple-scattering theory (MST) was originally formulated for the case of bulk solids by Korringa⁶³ and by Kohn and Rostoker⁶⁴ (KKR) and was further developed by other authors.^{65,66} The application to the calculation of LEED I/V curves within the LKRR method is clearly set forth in the book by Pendry,⁶⁰ while the extension to self-consistent total-energy calculations for surfaces and interfaces is contained in subsequent work.⁶⁷

The method to be presented in this paper provides an alternative solution to layer doubling for the calculation of the scattering (transition) matrix for a semi-infinite solid. The main differences between the two formalisms is the replacement of the plane-wave expansions of the interplanar propagator in conventional layer doubling methods with expansions in spherical waves, and the replacement of the layer doubling process itself with its numerically monitored convergence by a self-consistent equation for determining the scattering matrix of a half space. As is shown in this paper, our method can yield the exact band structure for any semi-infinite or doubly semi-infinite set of nonoverlapping real cell potentials in the limit $L \rightarrow \infty$, where L is a composite angular momentum index, $L = (l, \mu)$. In fact, numerical calculations indicate that convergence is reached at quite low values of L , of the order of 2 or 3 in the case of transition metals. In its present form, the theory is restricted to coherent interfaces, i.e., planar interfaces formed by materials based on the same crystal structure. Work currently in progress is aimed at removing this restriction. Even in its present restricted form, the method allows the calculation of the Green function for a variety of physically important systems such as adsorbed or absorbed atoms near surfaces, substitutional and/or interstitial impurities near surface and (coherent) interface regions, and twist and tilt grain boundaries, to name a few. Thus, formally it solves exactly the mathematical problem of electron scattering associated with semi-infinite systems or, in the case of coherent interfaces, or doubly semi-infinite materials,

formed by the repetition in either direction perpendicular to the surface or interface of a plane or a stack of planes.

In addition to the exact method, we also present a highly accurate scheme which for the case of semi-infinite solid surfaces yields results identical to those of the exact formalism, while being much simpler computationally. Both techniques are presented in the body of the paper and are illustrated with the results of calculations.

For the sake of simplicity of exposition we shall present our method for the case of monatomic lattices characterized by nonoverlapping MT potentials. The lifting of the MT approximation is currently under study by ourselves^{61,68} and by other investigators.^{62,69} Also, in the first presentation of the formalism we shall neglect some physically important effects such as lattice and/or potential relaxation near a surface or interface. It may become apparent from the present formalism how some of these effects can be treated. We do, however, present results based on the self-consistent determination of the spin-polarized charge densities of a (111) tilt grain boundary in Fe. The capability to calculate total energies is presently being developed.

The remainder of the paper takes the following form: Section II contains the basic formal ingredients upon which our method rests, including expressions for the multiple-scattering Green function, the scattering-path operator, and certain useful expansion properties of the free-particle propagator. The concepts of semi-infinite periodicity and of removal invariance are presented in Sec. III, while the formalism itself is given in Sec. IV. Section V contains a description of the treatment of surfaces and certain classes of interfaces within the embedded cluster method, and Sec. VI contains the results of numerical applications of the method to both model and realistic systems, along with a comparison with the results obtained using other methods. A final discussion of this work is then given in Sec. VI.

II. BASIC FORMALISM

In this section we present a number of basic concepts and establish a notation that will be used in our subsequent development. We begin with the MST equation of motion for the on-the-energy-shell scattering matrix, or scattering-path operator⁷⁰ for a collection of nonoverlapping MT potentials. This equation, which for the form of potentials chosen describes exactly the scattering properties of any collection of MT scatterers is the unifying feature in the treatment of finite clusters of scattering potentials, semi-infinite solids and bulk materials. Then, we present certain expansion properties of the free-particle propagator, which, in the next section, are used to describe the consistency condition for the scattering matrix of a semi-infinite solid.

A. The Green function and scattering matrix

The Green function for a collection of MT potentials (not necessarily spherically symmetric) is given⁶⁶ by the expression,

$$G^{ij}(\mathbf{r}, \mathbf{r}') = \sum_{L, L'} Z_L^i(\mathbf{r}) \tau_{LL'}^{ij} Z_{L'}^j(-\mathbf{r}') - \sum_L Z_L^i(\mathbf{r}) S_L^j(\mathbf{r}') \delta_{ij}, \quad (2.1)$$

where $\mathbf{r}(\mathbf{r}')$ are vectors in cells $i(j)$, and in the last term of this equation $|\mathbf{r}'|$ is chosen to be larger than $|\mathbf{r}|$. The function $Z_L^i(\mathbf{r})$ is the regular solution of the Schrödinger equation for the i th MT potential, which on the surface of the MT sphere joins smoothly to the function

$$Z_L^i(\mathbf{r}') = \sum_{L'} J_{L'}(\mathbf{r}') m_{L'L}^i - ik H_L(\mathbf{r}'). \quad (2.2)$$

The symbol $S_L^i(\mathbf{r})$ denotes that irregular solution for the potential in cell (MT) i , which on the surface of the MT sphere joins smoothly to $J_L(\mathbf{r})$. In Eq. (2.2), $m_{LL'}^i$ is the inverse of the scattering matrix for cell i , $\underline{m}^i = (\underline{t}^i)^{-1}$, in an angular momentum representation, while $J_L(\mathbf{r})$ and $H_L(\mathbf{r})$ denote the functions

$$J_L(\mathbf{r}) = j_l(kr) Y_L(\hat{\mathbf{r}}) \quad \text{and} \quad H_L(\mathbf{r}) = h_l^+(kr) Y_L(\hat{\mathbf{r}}), \quad (2.3)$$

where $j_l(kr)$ and $h_l^+(kr)$ are the spherical Bessel and outgoing Hankel functions, respectively, and $Y_L(\hat{\mathbf{r}})$ is a spherical harmonic or a linear combination of spherical harmonics which can be chosen to be real. As usual, $k = \sqrt{E}$, where E is a (generally complex) energy parameter. For a real energy, the site-diagonal part of $G(\mathbf{r}, \mathbf{r}')$, the second term in Eq. (2.1), can be made real and thus does not contribute to the charge density.

Our subsequent manipulations will be considerably simplified through the use of a vector-matrix notation in angular momentum space. In this notation symbols with single angular-momentum indices are denoted as bra (or ket) vectors, while matrices will be signified by underlines. A double underline will be used to denote a matrix in a mixed-site angular-momentum representation. In this notation, Eqs. (2.1) and (2.2) take the concise forms

$$G^{ij}(\mathbf{r}, \mathbf{r}') = \langle Z^i(\mathbf{r}) | \underline{\tau}^{ij} | Z^j(-\mathbf{r}') \rangle - \langle Z^i(\mathbf{r}) | S^j(\mathbf{r}') \rangle \delta_{ij} \quad (2.1a)$$

with $|\mathbf{r}'| > |\mathbf{r}|$ and $\mathbf{r}(\mathbf{r}')$ in cells $i(j)$, and

$$\langle Z^i(\mathbf{r}) | = \langle J(\mathbf{r}) | \underline{m}^i - ik \langle H(\mathbf{r}) |. \quad (2.2a)$$

Clearly the use of these equations requires the knowledge of the functions $|Z^j(\mathbf{r})\rangle$ and of the site matrix elements, $\underline{\tau}^{ij}$, of the scattering-path operator. The former can be found through the solution of the Schrödinger equation for the (self-consistent) potential in cell i , which can be accomplished by means of well-known procedures. (We note that the *self-consistent* determination of the potential in cell i requires only the knowledge of the site-diagonal element, $\underline{\tau}^{ii}$.) These procedures also determine the individual scattering matrices,⁷¹⁻⁷³ for cell (MT) i , which in our presentation will be treated as being known. Given these scattering matrices it remains to determine the scattering-path operator $\underline{\tau}^{ij}$, whose matrix elements satisfy⁷⁰ the equation of motion:

$$\underline{\tau}^{ij} = \underline{t}^i \delta_{ij} + \underline{t}^i \sum_{k \neq i} \underline{G}^{ik} \underline{\tau}^{kj}. \quad (2.4)$$

Here, the quantities $\underline{G}_{ik} \equiv \underline{G}(\mathbf{R}_k - \mathbf{R}_i)$ are the site-matrix elements in an angular-momentum representation of the free-particle propagator and are, therefore, the real-space representatives of the familiar KKR structure constants. (Explicit expressions for \underline{G}^{ij} can be found⁷⁴ in the literature are also summarized in the next subsection.) As will be seen in the following exposition, certain expansion properties of these coefficients are a major building block of the formalism.

Equation (2.4) is exact as it stands and is applicable to any system of MT potentials, including reduced-symmetry systems. For materials characterized by full three-dimensional periodicity, Eq. (2.4) can be solved by means of lattice Fourier transforms yielding solutions of the well-known KKR type. For systems with reduced symmetry, such as surfaces and interfaces, Eq. (2.4) must be treated by other means. In any case, once \underline{t} , and hence $G(\mathbf{r}, \mathbf{r}')$, have been determined, all single-particle properties of the scattering assembly, e.g., charge densities and densities of states, can be obtained through well-known expressions.^{74,75}

In this paper we are concerned with the solution of Eq. (2.4) in connection with planar surface and coherent interface regions formed by pure elemental solids. These systems are based on structures exhibiting two-dimensional periodicity in which case the concept of lattice Fourier transforms in two-dimensional reciprocal space can be used to advantage. We consider a semi-infinite solid as consisting of planes of atoms characterized by a scattering center, α , arranged on the points, \mathbf{R}_α of a two-dimensional lattice. In the case of one atom per two-dimensional unit cell, we label atom i as (α, I) , which denotes atom α in plane I . Upon introducing the lattice Fourier transforms,

$$\underline{\tau}^{IJ}(\mathbf{k}) = \sum_{\alpha} e^{i\mathbf{k} \cdot \mathbf{R}_\alpha} \underline{\tau}^{0I\alpha J} \quad (2.5)$$

and

$$\underline{G}^{IJ}(\mathbf{k}) = \sum_{\alpha} e^{i\mathbf{k} \cdot \mathbf{R}_\alpha} \underline{G}^{0I\alpha J}, \quad (2.6)$$

where the prime excludes $\alpha=0$ if $I=J$, and \mathbf{k} is a vector in the reciprocal lattice defined by the periodicity of a surface (or interface), we can write,

$$\underline{\tau}^{IJ}(\mathbf{k}) = \underline{t}^I(\mathbf{k}) \delta_{IJ} + \underline{t}^I(\mathbf{k}) \sum_{K \neq I} \underline{G}^{IK}(\mathbf{k}) \underline{\tau}^{KJ}(\mathbf{k}). \quad (2.7)$$

In the case of polyatomic two-dimensional unit cells, a further index may be necessary in order to distinguish inequivalent atoms. We note that the restriction in the sum of Eq. (2.7) is consistent with the definition

$$\underline{m}^I(\mathbf{k}) = \underline{m}^I - \underline{G}^{II}(\mathbf{k}), \quad (2.8)$$

with \underline{m}^I being the inverse of the scattering matrix characterizing plane I , $\underline{m}^I = (\underline{t}^I)^{-1}$, and $\underline{G}^{II}(\mathbf{k})$, the intraplanar free-particle propagator associated with plane I . These, and the interplanar Green functions, $\underline{G}^{IJ}(\mathbf{k})$, can be evaluated using techniques presented by Kambe.⁷⁶ As it stands, the "one-dimensional" Eq. (2.7) provides a particularly convenient expression for the study of extended defects with two-dimensional periodicity.

B. Expansions of G^{ij}

We begin by recalling the expansion properties of the functions $|J(\mathbf{r})\rangle$ and $|H(\mathbf{r})\rangle$ under a shift of the origin. It can be readily be shown⁷⁷ that

$$|J(\mathbf{r}+\mathbf{a})\rangle = \underline{g}(\mathbf{a})|J(\mathbf{r})\rangle \quad \text{for all } \mathbf{r} \text{ and } \mathbf{a} \quad (2.9)$$

and

$$|H(\mathbf{r}-\mathbf{a})\rangle = \underline{g}(\mathbf{a})|H(\mathbf{r})\rangle \quad \text{for } |\mathbf{r}| > |\mathbf{a}| \quad (2.10a)$$

or

$$|H(\mathbf{r}-\mathbf{a})\rangle = \widehat{G}(\mathbf{a})|J(\mathbf{r})\rangle \quad \text{for } |\mathbf{r}| < |\mathbf{a}|. \quad (2.10b)$$

The coefficients $\underline{g}(\mathbf{a})$ and $\widehat{G}(\mathbf{a})$ are given explicitly by the expressions

$$[\underline{g}(\mathbf{a})]_{LL'} = 4\pi \sum_{L''} i^{l-l'+l''} C(LL'L'') J_{L''}(\mathbf{a}) \quad (2.11)$$

and

$$[\widehat{G}(\mathbf{a})]_{LL'} = 4\pi \sum_{L''} i^{l-l'+l''} C(LL'L'') H_{L''}(\mathbf{a}), \quad (2.12)$$

with the latter quantity being proportional to the real-space KKR structure constants, $\underline{G}(\mathbf{a}) = -ik\widehat{G}(\mathbf{a})$. The symbols $C(LL'L'')$ denote the usual Gaunt numbers. It follows easily from these equations that

$$\underline{g}(\mathbf{a})\underline{g}(-\mathbf{a}) = \underline{g}(-\mathbf{a})\underline{g}^+(\mathbf{a}) = \underline{1} \quad (2.13)$$

and

$$\begin{aligned} \underline{G}(\mathbf{R}-\mathbf{a}) &= \underline{G}(\mathbf{R})\underline{g}(\mathbf{a}) \\ &= \underline{g}(\mathbf{a})\underline{G}(\mathbf{R}) \quad \text{for } |\mathbf{R}| > |\mathbf{a}|. \end{aligned} \quad (2.14)$$

The matrices $\underline{g}(\mathbf{a})$ are simply the angular-momentum representation of the translation operator. It is interesting to note that it is possible to expand $\underline{G}(\mathbf{R}-\mathbf{a})$ in terms of $\underline{G}(\mathbf{R})$ even when $|\mathbf{a}| > |\mathbf{R}|$. In this case we may consider a stepwise process based upon the property that *any* vector \mathbf{a} can be written as a sum of n vectors \mathbf{a}_α such that $|\mathbf{R} - \sum_{\alpha=1}^n \mathbf{a}_\alpha| > |\mathbf{a}_{n+1}|$. This is always possible and leads to the expansion

$$\underline{G}(\mathbf{R}-\mathbf{a}) = \underline{g}(\mathbf{a}_n) \{ \underline{g}(\mathbf{a}_{n-1}) \cdots \underline{g}(\mathbf{a}_2) [\underline{g}(\mathbf{a}_1) \underline{G}(\mathbf{R})] \},$$

where the brackets indicate that $\underline{g}(\mathbf{a}_1)$ and $\underline{G}(\mathbf{R})$ are multiplied first to produce $\underline{G}(\mathbf{R}-\mathbf{a}_1)$, then $\underline{g}(\mathbf{a}_2)$ is multiplied with $\underline{G}(\mathbf{R}-\mathbf{a}_1)$ to produce $\underline{G}(\mathbf{R}-\mathbf{a}_1-\mathbf{a}_2)$, and so on. In other words, this process allows one to obtain $\underline{G}(\mathbf{R}-\mathbf{a})$ by expanding around rather than through the pole of the Green function at $\mathbf{R}=\mathbf{a}$. We denote this inherently convergent multiplication process by the symbol \odot , so that we can write

$$\underline{G}(\mathbf{R}-\mathbf{a}) = \underline{g}(\mathbf{a}) \odot \underline{G}(\mathbf{R}) \quad \text{for all } \mathbf{R} \text{ and } \mathbf{a} \quad (2.15)$$

III. SEMI-INFINITE PERIODICITY AND REMOVAL INVARIANCE

Equation (2.7) can be viewed as representing a semi-infinite chain of scattering potentials, each represented by

the ‘‘planar’’ scattering matrices defined in Eq. (2.8). As such, it provides one of the simplest examples of a system characterized by semi-infinite periodicity (SIP), which we define in general as *the periodic repetition of a basic scattering unit, e.g., a monolayer, along a given direction*. It is almost self evident that systems characterized by SIP possess the following property of *removal invariance*, namely, that *the scattering properties of such systems remain unchanged when a finite number of basic repeating units is removed from the free end of the system*.

The concepts of SIP and of removal invariance can be used⁷⁸ to formulate multiple-scattering theory entirely within direct (real) rather than reciprocal space. In the next section, they are used to derive a \mathbf{k} -dependent form of the equation satisfied by the scattering-path operator of a semi-infinite periodic solid.

IV. THE SCATTERING-PATH OPERATOR FOR A SEMI-INFINITE PERIODIC SOLID

Let \underline{T} denote the total scattering matrix of a semi-infinite periodic arrangement of scattering units, expanded about the center of the first unit, with each unit characterized by the scattering matrix $\underline{t}^I \equiv \underline{t}$. Because of the property of removal invariance of such a system, \underline{T} remains unchanged when an integral number N_b of basic units is removed from the free end of the system. Thus, a system consisting of $N_b + 1$ cells with N_b basic units and a renormalized cell with scattering matrix \underline{T} at the $(N_b + 1)$ th position must be describable by the same scattering matrix \underline{T} . It is now possible to replace a system consisting of an infinite number of scattering cells by a cluster of a finite number of cells, with the cell at the boundary site properly renormalized, or ‘‘dressed,’’ to represent the material extending to infinity beyond the cluster. This gives rise to the self-consistent equation^{78,79}

$$\underline{T} = \sum_{I,J} \underline{g}(-\mathbf{R}_{0I}) \underline{t}^{IJ}(\underline{T}) \underline{g}(-\mathbf{R}_{J0}) \quad (4.1)$$

determining the scattering matrix \underline{T} , and hence, \underline{t}^{IJ} , for the system under consideration. In the case being considered here, both \underline{T} and \underline{t}^{IJ} are \mathbf{k} dependent, while $\underline{g}(\mathbf{R}_{IJ})$ is the \mathbf{k} -independent element of the translation operator in the angular-momentum representation, Eq. (2.11), corresponding to the vector \mathbf{R}_{IJ} . The matrix $\underline{t}^{IJ}(\underline{T})$ in Eq. (4.1) can be obtained as the inverse of the matrix

$$\underline{M}^{IJ} = \left\{ \begin{array}{ll} \underline{m}^I(\mathbf{k})\delta_{IJ} & I=J \neq N_b+1 \\ [\underline{T}(\mathbf{k})]^{-1}\delta_{IJ} & I=J=N_b+1 \\ -\underline{G}^{IJ}(\mathbf{k})(1-\delta_{IJ}) & I \neq J \end{array} \right\} \quad (4.2)$$

in which the \mathbf{k} dependence of the various quantities is explicitly shown on the right-hand side. This equation exhibits the self-consistent nature of Eq. (4.1), showing that the inverse of \underline{t} contains \underline{T} in the $(N_b + 1)$ th position.

It is a matter of some straightforward, although occasionally tedious, algebra to show that Eq. (4.1) can be written in a number of formally equivalent forms. These different forms, however, may exhibit considerably different numerical behavior because of the truncations in

the angular-momentum expansions in Eq. (4.1), which are necessary in realistic three-dimensional calculations. A particularly convenient form of the self-consistent equation can be obtained in terms of the scattering-path operator $\underline{\tau}$ itself. In the spirit of the real-space multiple-scattering theory (RS-MST) method, we represent the scattering-path operator, corresponding to a semi-infinite collection of scattering centers by an effective matrix $\underline{\bar{\tau}}$, corresponding to a finite number of scatterers with the boundary sites renormalized so as to simulate the presence of the semi-infinite material. The self-consistent equation for $\underline{\bar{\tau}}$ takes the form

$$\underline{\bar{\tau}} = \begin{pmatrix} \underline{1} & \underline{0} & \cdots & \underline{0} & \underline{0} \\ \underline{0} & \underline{1} & \cdots & \underline{0} & \underline{0} \\ \vdots & \vdots & \ddots & \vdots & \vdots \\ \underline{0} & \underline{0} & \cdots & \underline{1} & \underline{g}(\mathbf{R}_{01}) \end{pmatrix} \begin{pmatrix} \underline{m} & -\underline{G} \\ -\underline{G}' & \underline{\bar{\tau}}^{-1} \end{pmatrix}^{-1} \times \begin{pmatrix} \underline{1} & \underline{0} & \cdots & \underline{0} \\ \underline{0} & \underline{1} & \cdots & \underline{0} \\ \vdots & \vdots & \ddots & \vdots \\ \underline{0} & \underline{0} & \cdots & \underline{1} \\ \underline{0} & \underline{0} & \cdots & \underline{g}(\mathbf{R}_{10}) \end{pmatrix}, \quad (4.3)$$

where \underline{m} is the inverse scattering matrix for the basic repeating unit, e.g., a plane, and \underline{G} (\underline{G}') are matrices formed from the interlayer structure constants between the layer or layers represented by \underline{m} and those represented by $\underline{\bar{\tau}}$. Explicitly, these quantities are given by the expressions

$$\underline{G} = (\underline{G}^{01}, \underline{G}^{02}, \dots, \underline{G}^{0n}) \quad (4.4a)$$

and

$$\underline{G}' = \begin{pmatrix} \underline{G}^{10} \\ \underline{G}^{20} \\ \vdots \\ \underline{G}^{n0} \end{pmatrix}, \quad (4.4b)$$

where \underline{G}^{IJ} are the \mathbf{k} -dependent, interlayer structure constants entering Eq. (2.7). It is a matter of some straightforward algebra to show that the multiple-scattering expansion of Eq. (4.3) gives an exact treatment of the scattering off the $(n+1)$ th plane away from the surface where n is the number of site indices in $\underline{\tau}$. In numerical implementations of Eq. (4.3), it is convenient to replace $\underline{G}(\mathbf{R}_{01})$ by the \mathbf{k} -dependent effective translation operator

$$\underline{g}(\mathbf{R}_{01}) = [\underline{G}^{0n}(\mathbf{k})]^{-1} [\underline{G}^{0,n+1}(\mathbf{k})] \quad (4.5)$$

with a similar construct for $\underline{g}(\mathbf{R}_{10})$. The advantage of this replacement is the virtual elimination of convergence difficulties that may be associated with the use of \underline{g} and the truncation of the angular-momentum expansions. We note that the effect of Eq. (4.3) is to add a bare layer, represented by \underline{m} , to the free end of a system with SIP, while "folding" the boundary site onto the one preceding it [note the structure of the bottom right-hand corners of the matrices that include the \underline{g} 's and compare with Eq. (4.1)]. We refer to this form of the self-consistent equation as the "folding mode."

Once the scattering-path operators, $\underline{\bar{\tau}}^L$ and $\underline{\bar{\tau}}^R$, for two

semi-infinite solids have been determined, the scattering-path operator for the interface formed by these two materials, and which may contain a number of impurity layers, is obtained as the inverse of the multiple-scattering matrix

$$\underline{\bar{\tau}}^{-1} = \begin{pmatrix} (\underline{\tau}^L)^{-1} & -\underline{G}^{Li} & -\underline{G}^{Ri} \\ -\underline{G}^{iL} & \underline{m}^i & -\underline{G}^{iR} \\ -\underline{G}^{RL} & -\underline{G}^{Ri} & (\underline{\bar{\tau}}^R)^{-1} \end{pmatrix}, \quad (4.6)$$

where \underline{m}^i is the inverse of the scattering matrix describing the interfacial impurity layers. In the case of surface calculations, the quantity $\underline{\tau}^L$ could represent the scattering off a surface barrier.

Once $\underline{\tau}^{IJ}(\mathbf{k})$ for a given plane and a given system has been determined, the corresponding electronic densities of states can be found from the expression [see Eq. (2.1a)]

$$\rho^I(\mathbf{k}, E) = -\frac{1}{\pi} \text{Im} G^{II}(\mathbf{k}, E) \\ = -\frac{1}{\pi} \text{Im} \int d^3r \langle Z(\mathbf{r}) | \underline{\tau}^{II}(\mathbf{k}) | Z(-\mathbf{r}) \rangle. \quad (4.7)$$

An integral over the variable \mathbf{k} confined to the first Brillouin zone (BZ) of the reciprocal lattice defined by the structure of the surface or interface yields the density of states in real space, $\rho^I(E)$.

V. THE TREATMENT OF SURFACES WITHIN THE EMBEDDED CLUSTER METHOD

The formalism presented in the last two sections is exact, yielding the proper scattering matrix associated with ideal semi-infinite periodic solids. At the same time, obtaining the solution of the self-consistent Eq. (4.6) may be computationally tedious.

Although the general formalism may be necessary in the study of general physical problems, a large number of important and interesting questions may be addressed within a conceptually and computationally simpler methodology. For example, the study of the electronic structure of surfaces can be considerably simplified if the vacuum potential barrier (work function) is taken into account. The simplifications result because of the inability of the electrons in the material to penetrate too deeply into the vacuum. Also, the treatment of stacking faults in an otherwise translationally invariant material can be undertaken within a computationally simple approach. In this section we propose a highly accurate and practicable method for the study of a certain class of two-dimensional defects in a periodic system. This method is based on the embedded cluster formalism,⁸⁰ and will be presented explicitly for the case of semi-infinite solids. The formalism, however, will be applicable in an essentially unchanged form to other types of defects, such as stacking faults. The main advantage of this formalism is that it obviates both the need for expansions in terms of the \underline{g} matrices and the necessity for solving a consistency equation for $\underline{\tau}$. Instead, the needed $\underline{\tau}^{IJ}$ are determined in terms of quantities associated with the underlying *bulk* periodic materials, which are much easier to calculate.

At the same time, this method rests upon the evaluation of one-dimensional integrals of quantities depending on the \mathbf{k} -dependent three-dimensional structure constants, and care should be exercised in its application.

As a simple model of a real surface, we consider the presence of a work function in the form of a potential barrier confining the electrons to the material. The interface formed by the constant vacuum barrier on one side and the material on the other can certainly be treated within the formalism of the previous sections. At the same time a much simpler approach becomes evident. Since electrons can hardly penetrate into the barrier, a slab of vacuum a few layers thick may be sufficient to separate the material into two semi-infinite parts, each part possessing quite closely the properties of a truly semi-infinite solid. With interference effects between opposite faces of the slab eliminated, or minimized, the treatment of a slab of vacuum embedded in a material satisfies the proper boundary conditions at infinity. As our model calculations reveal, this treatment is essentially exact for energies below the barrier with only a few vacuum layers, 3–5, included in the slab.

Within the embedded-cluster method (ECM),⁸⁰ one defines the renormalized interactor $\underline{\underline{A}}^C$ associated with a cluster of sites, C , describing the interaction of these sites with the surrounding medium. $\underline{\underline{A}}^C$ can be obtained in terms of the cluster t matrix and scattering-path operator,

$$\underline{\underline{A}}^C = (\underline{t}^C)^{-1} - (\underline{\underline{t}}^{CC})^{-1}. \quad (5.1)$$

This expression can be readily applied to the one-dimensional, \mathbf{k} -dependent Eq. (2.7). In this case, we have

$$\{[\underline{t}^C(\mathbf{k})]^{-1}\}_{IJ} = [\underline{m} - \underline{G}^{IJ}(\mathbf{k})]\delta_{IJ} - \underline{G}^{JJ}(\mathbf{k})(1 - \delta_{IJ}), J \in C \quad (5.2)$$

and

$$[\underline{\underline{t}}^{CC}(\mathbf{k})]_{IJ} = \frac{1}{\Omega_Z} \int_{\Omega_Z} \bar{\underline{t}}(\mathbf{k}_b) e^{ik_z(z_I - z_J)} dk_z, \quad (5.3)$$

where \underline{m} and $\underline{G}^{IJ}(\mathbf{k})$ are defined in Eqs. (2.8), the vectors \mathbf{k} are confined to the two-dimensional BZ, \mathbf{k}_b is a reciprocal lattice vector of the *bulk* solid, and the integration extends through the region Ω_z of the z component of \mathbf{k}_b . The quantity $\bar{\underline{t}}(\mathbf{k}_b)$ denotes the scattering-path operator of the bulk material. Using Eqs. (5.1)–(5.3) we can write the scattering-path operator associated with a stack of impurity planes, such as a vacuum slab, in the form

$$\underline{\underline{t}}^{CC}(\mathbf{k}) = \{ \underline{m}^I(\mathbf{k}) - \underline{m}(\mathbf{k}) + [\bar{\underline{t}}^{CC}(\mathbf{k})]^{-1} \}^{-1}. \quad (5.4)$$

Planes adjacent to the vacuum slab can be incorporated into the impurity cluster and studied through Eq. (5.4). Finally, the real-space matrix elements $\underline{\underline{t}}$ can be obtained through the formalism of Sec. IV.

VI. NUMERICAL RESULTS

We have used the formalism of the preceding sections to calculate surface and interface density-of-states (DOS) curves for model one-dimensional systems and for three-dimensional realistic materials described by MT poten-

tials. One-dimensional systems are particularly convenient as a testing ground of the formalism presented in this paper because the expansions in angular momentum eigenstates include only two states, $L=0$ and 1, and can be carried to convergence. Thus, the formalisms of the previous sections can be implemented exactly in terms of two-dimensional matrices. Clearly, no \mathbf{k} dependence arises in the treatment of one-dimensional materials within the present formalism. For completeness of presentation we exhibit Figs. 1 and 2 which were originally reported in Ref. 79.

The three-dimensional calculations presented clearly indicate the rapid convergence that can be achieved through the use of Eqs. (4.3) and (4.4). They also illustrate that this equation can be used to treat high Miller-index surfaces and interfaces, such as stepped surfaces characterized by small interplanar separations. Thus, this method provides a viable and more flexible alternative to the layer doubling method, which can be used reliably only for the study of low Miller-index surfaces.

A. One-dimensional systems

An example of the cell potential used in this part of our study is shown in Fig. 1. The upper frame in this figure

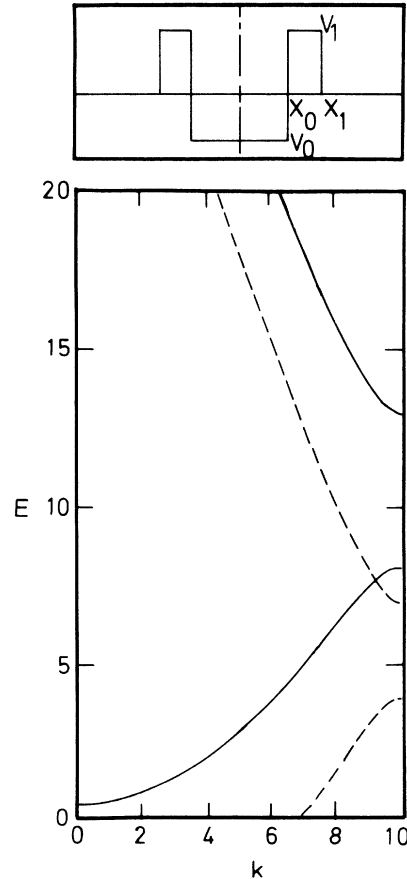


FIG. 1. One-dimensional potential well with shoulders and the associated band structure for two different choices of such potentials. Solid curve: $X_0=0.4$, $X_1=0.5$, $V_0=-2.0$, $V_1=12.0$; dashed curve: $X_0=0.4$, $X_1=0.5$, $V_0=-6.0$, $V_1=2.0$.

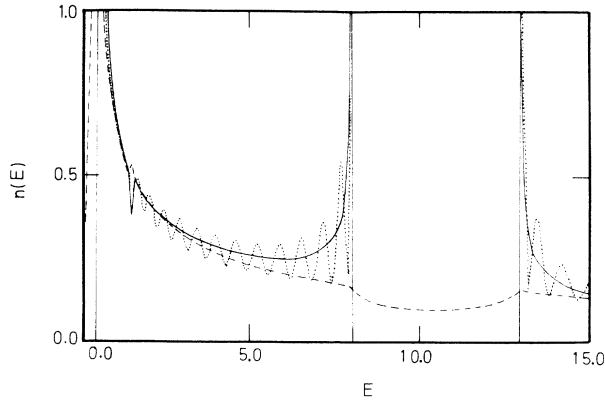


FIG. 2. Local densities of states for one-dimensional infinite and semi-infinite systems. The solid curve represents the DOS for an infinite (bulk) arrangement of potentials of the kind exhibited in Fig. 3 for the values $X_0=0.4$, $X_1=0.5$, $V_0=2.0$, and $V_1=12.0$. The dashed curve is the DOS at the surface site of a semi-infinite arrangement of such potentials, and the dotted curve represents the DOS at the 20th site beneath the surface of a semi-infinite one-dimensional chain.

depicts a one-dimensional cell potential, while the lower frame shows the band structures associated with periodic, linear arrays of such potentials for two different values of the potential parameters, as specified in the caption.

The DOS associated with both infinite and semi-infinite one-dimensional systems characterized by the cell potential shown in Fig. 1 are depicted in Fig. 2. The DOS for an infinite (bulk) material is shown by the continuous curve and clearly exhibits the gap present in the band structure of the material, Fig. 1. The dashed curve in the figure depicts the local DOS at the surface site of a semi-infinite system. The DOS was calculated from the imaginary part of the Green function at the surface site with structural and potential reconstruction effects ignored (ideal surface). As might be expected, the surface DOS quite closely resembles that for free electrons, reflecting the freedom of electrons to leak away into the vacuum, $V=0$, region. The dotted curve in Fig. 2 shows the local DOS at the 20th site below the surface. As is seen here, the gap is fully reproduced, while the remainder of the DOS twines around the bulk DOS in a manner characteristic of one-dimensional systems. The oscillations can be expected to die out much more rapidly with distance away from the surface in realistic three-dimensional materials, particularly metals, where the coordination number is greater than for one-dimensional systems and screening effects are much more prominent.

Interface DOS associated with two semi-infinite materials of the type depicted in Figs. 1 and 2 joined together are shown in Fig. 3. In all cases, the potential parameters characterizing the materials are given in the figure captions. The continuous curves in the figure depict the bulk DOS of the material referred to in connection with Figs. 1 and 2, material 1, while the dashed curves correspond to the bulk DOS for different choices of the potential characterizing material 2. The dotted curve is the

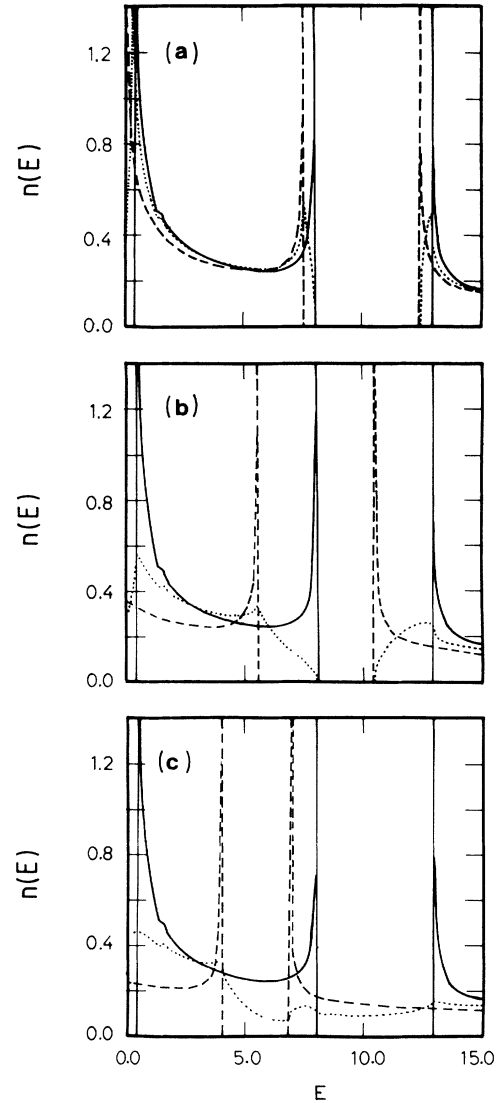


FIG. 3. Bulk and interface DOS for one-dimensional systems. In all panels, the solid curve represents the DOS for an infinite arrangement of potentials of the kind exhibited in Fig. 3 for the choice $X_0=0.4$, $X_1=0.5$, $V_0=-2.0$, and $V_1=12.0$. The dotted curve is the DOS on a site occupied by such a potential adjacent to an interface formed with a semi-infinite system characterized by the choices $V_0=-2.5$, $V_1=11.5$ in (a), $V_0=-4.5$, $V_1=9.5$ in (b), and $V_0=-6.0$, $V_1=2.0$ in (c).

DOS associated with a cell of material 1 adjacent to the interface. The potentials chosen for material 2 allow a rather detailed study of the interface DOS as a function of gap overlap. As is seen in this figure, the interface DOS always vanishes in regions in which both bulk materials form a gap, and, as may be expected, reflects only weakly the presence of the Van Hove singularities of the infinite systems. The interface DOS shows no gap in the case in which no common region exists in which both bulk DOS vanish, Fig. 3(c).

We have checked the accuracy of our codes by using them to calculate bulk DOS for one-dimensional systems,

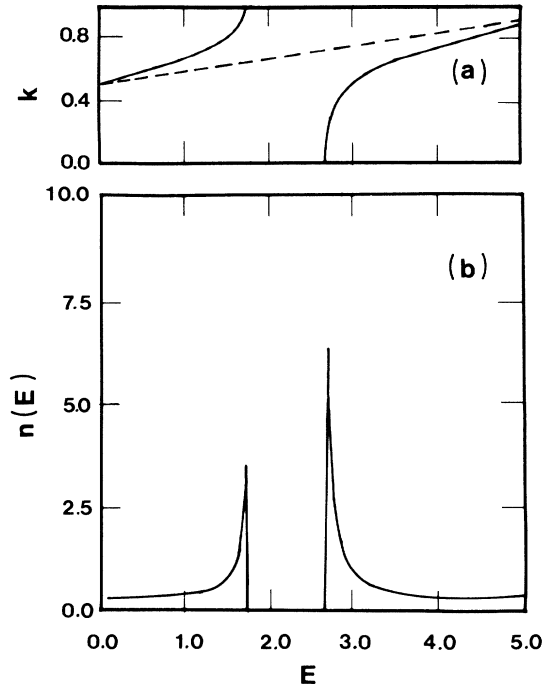


FIG. 4. Band structure, (a) and DOS (b) for an infinite one-dimensional array of potentials described by parametrized phase shifts, after Butler (Ref. 81).

which can be accomplished through the use of Eq. (4.6). In all cases we found results identical, within numerical accuracy, to those obtained through an application of the KKR formalism, i.e., through the use of Fourier transforms.

In order to gain some insight into the properties of realistic, three-dimensional materials by means of simple one-dimensional model calculations, Butler⁸¹ introduced a parametrized set of phase shifts, which exhibit a reso-

nance in the $L=1$ channel. In this model the phase shifts are assumed to be of the form

$$\tan\delta_0 = \lambda/\sqrt{E}, \quad \tan\delta_1 = \Gamma/(E - E_0) + \Gamma/E.$$

Figure 4 is essentially identical to that exhibited by Butler, and shows the band structure and corresponding DOS for a particular choice of the parameters describing the phase shifts. In our calculations we chose the same parameters as Butler,⁸¹ $\lambda=2.0$, $E_0=2.05$, $\Gamma=0.50$ with all energies in arbitrary units and also introduced a potential barrier with respect to the vacuum in the form of a potential step whose height, V_b , could be varied arbitrarily.

Figure 5 depicts the bulk DOS, in 5(a), the local DOS on a site next to the interface with the vacuum barrier $V_b=5.0$, calculated using the exact interface condition, Eq. (3.8), in 5(b), and the DOS on the interface calculated by inserting a cluster (slab) consisting of five vacuum layers, also in 5(b). It is to be emphasized that the last two approaches yield identical results. This result justifies both approaches, at least with respect to the systems under study, and increases our confidence in both the exact method, Eq. (3.8), and that based on the embedded cluster approach. As is seen in this figure, the perturbation caused by the presence of the vacuum barrier destroys the Van Hove singularities and introduces a surface state in the gap of the infinite system. This is to be compared with the behavior of the DOS at a free surface, $V_b=0$, shown by the dotted curve in Fig. 6. The solid curve in Fig. 6 is the bulk DOS and is identical to that exhibited by Butler,⁸¹ and also shown in Fig. 4.

Using this simple parametrized model, we examined the behavior of the surface state in Fig. 5 with respect to barrier height and with respect to distance from the interface. The corresponding results are shown in Figs. 7 and 8, obtained using the numerically equivalent but computationally easier approach of embedding a vacuum slab in the solid. As is seen in Fig. 7 increasing the height of the

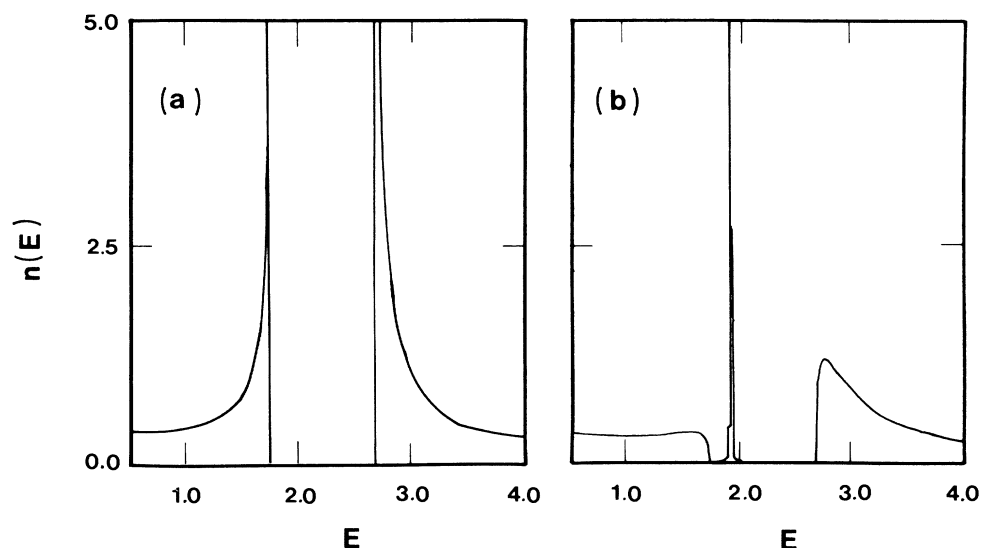


FIG. 5. Bulk (a) and interface densities of states (b) and (c) for the one-dimensional parametrized model. DOS in (b) were calculated using the exact formalism, whereas those in (c) were obtained using the ECM, both with a barrier height $V_b=5.0$.

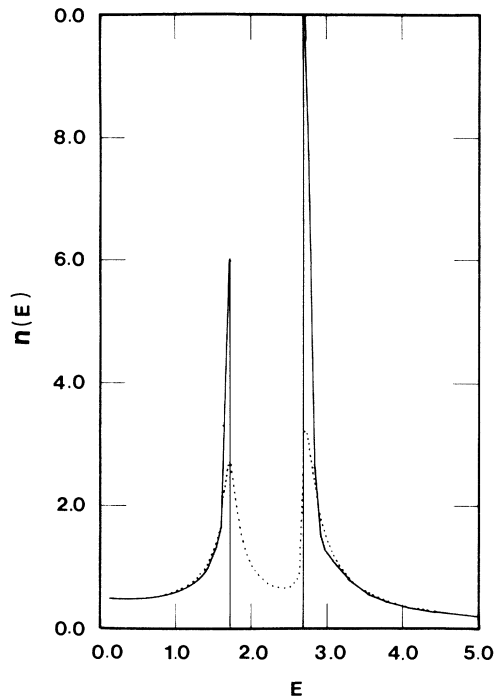


FIG. 6. Bulk (solid curve) and free surface (dotted curve) DOS for the one-dimensional parametrized model obtained using the exact formalism of Sec. III.

vacuum step causes all states, including the surface states, to recede to higher energies. The movement of the band states towards higher energies manifests itself in a drop in the DOS near the gap. This behavior can be expected, since only states with relatively high energy could possess appreciable amplitude near a positive potential barrier.

The localized nature of the surface states is clearly illustrated in Fig. 8. As the distance from the surface in-

creases, the gap states lose weight and practically disappear even at the second site below the surface. The local DOS at the 20th site below the surface quite closely resembles the bulk DOS, exhibiting the one-dimensional oscillations we encountered in Fig. 2, and containing no remnant of the states in the gap.

B. Three-dimensional systems

An isolated $\Sigma 3$ (111) tilt grain boundary in Fe has been studied using the techniques discussed above. The boundary is formed by joining two semi-infinite stacks of (111) planes together and the resulting structure is shown in Fig. 9. The calculations are based on fully self-consistent spin-polarized charges, obtained by allowing the potential to relax in the first five layers on either side of the boundary plane, while keeping the potential in planes deeper into the material equal to its bulk value. Each self-consistent iteration took approximately 20 min on a VAX 8600, and as with most magnetic systems several hundred iterations were performed in order to assure convergence.

The semi-infinite stacks of (111) planes used to embed the interface region were represented by two renormalized scattering matrices, i.e., \bar{T}^R and \bar{T}^L in Eq. (4.6), and only partial waves up to $l=2$ were included in an angular momentum expansion. The total charge density was found by integrating the local density of states over energy, which was in turn obtained through integration over two-dimensional (2D) Brillouin zone. The former was evaluated by contour methods using eight points along the contour, and the latter with six special k points. Further details on the self-consistent solution for \bar{T} and the determination of the charge density can be found in the literature.^{67,82}

The density of states for the majority and minority spin bands are shown in Fig. 10, as a function of the layer away from the interface plane. The DOS for bulk Fe is also shown for comparison. As is seen in this figure, the DOS of the majority band at the interface, labeled plane

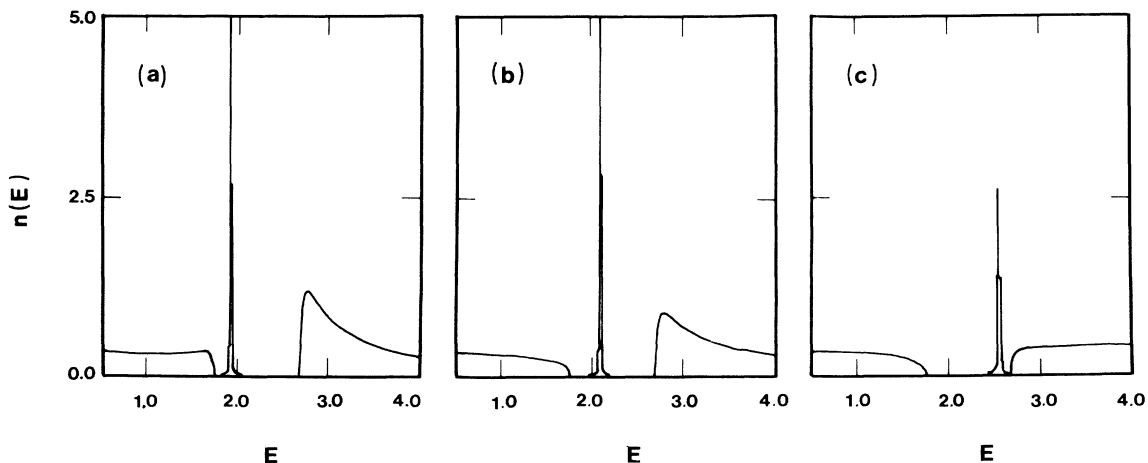


FIG. 7. Behavior of surface state with increasing barrier height. $V_b = 5.0$ (a), $V_b = 10.0$ (b), and $V_b = 100.0$ (c) for the one-dimensional parametrized model.

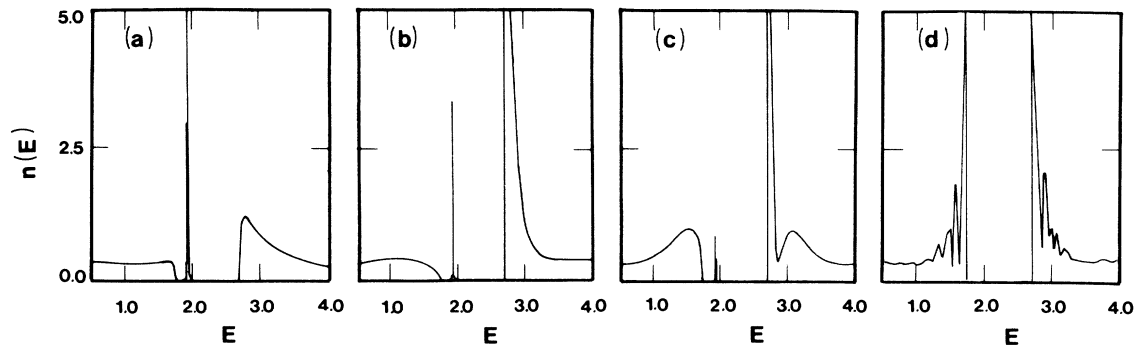


FIG. 8. Local DOS as a function of distance from the interface with a barrier of height $V_b = 5.0$, for the parametrized one-dimensional model. (a), (b), (c), and (d) depict, respectively, the DOS at the surface site, and at the second, third, and 20th sites away from the interface.

gb in the figure, exhibits significant localization, with d -band narrowing resulting from the reduced atomic coordination. The electronic structure is perturbed over several layers away from the interface, although most bulk features are recovered on the second layer, plane -2 , away from the interface.

In both majority and minority DOS, there are significant perturbations mainly around the Fermi energy. As a consequence of a nearly full majority band on the boundary layer there results a significantly enhanced moment over the bulk value. The DOS profiles of this boundary layer are in fact similar to those obtained in a Fe monolayer,⁸³ presumably because of the decreased coordination around the interface layer.

These preliminary calculations on a realistic grain boundary show that the approach presented in this paper is both convergent and computationally efficient. The fact that the method yields converged results in the case of (111) Fe grain boundaries, in which the interplanar separation is fairly small, ($< 1 \text{ \AA}$) is an indication of the applicability of this method to the study of high Miller-index surfaces and interfaces. Further work presently underway is aimed at the determination of the energetics of grain boundaries, and the effect of impurities on the magnetic and mechanical properties of interfaces.

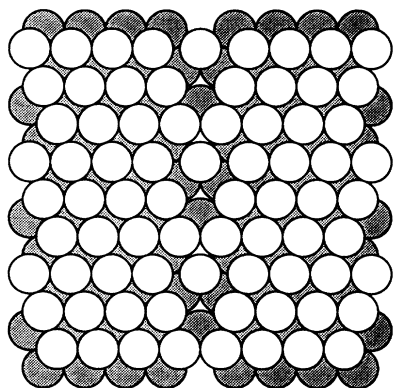


FIG. 9. Atomic structure at a Σ_3 tilt grain boundary in Fe.

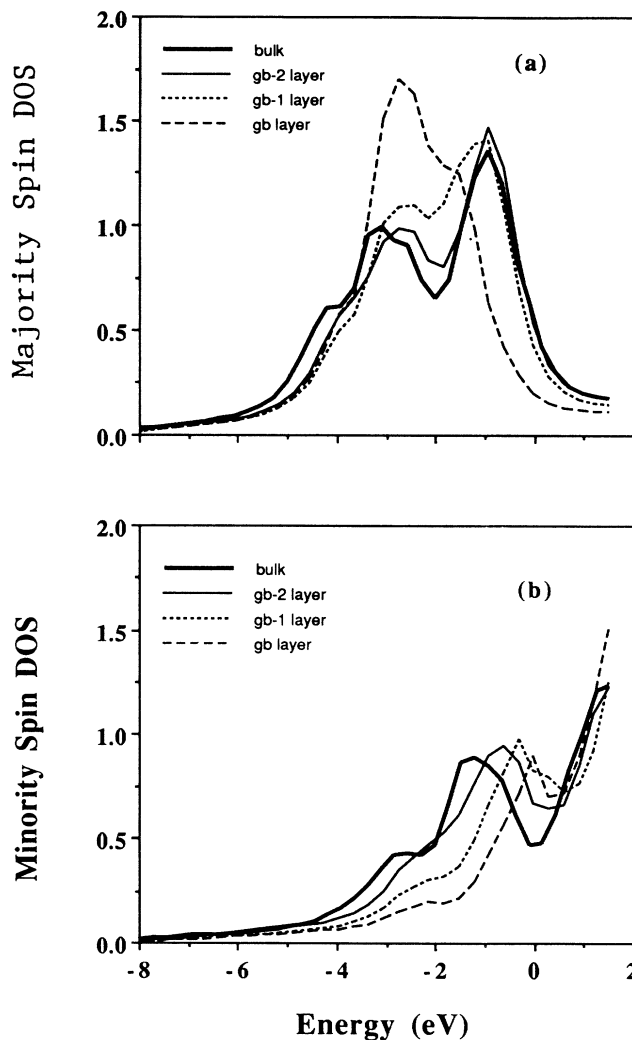


FIG. 10. Densities of states per atom per eV for majority (a) and minority (b) boundary layers, labeled gb, layer adjacent to the boundary, labeled -1 , and two layers away from the boundary, labeled -2 . The bulk DOS is also shown for comparison.

VII. DISCUSSION AND CONCLUSIONS

In this paper we have introduced new formal methods, based on multiple scattering theory, for the treatment of the electronic structure of surfaces and coherent interfaces. We tested our methods numerically in connection with model one-dimensional systems and demonstrated their flexibility and accuracy as well as the similarities and differences between the various formal approaches. We also presented fully charge self-consistent calculations for Fe, illustrating the practical applicability of our approach. One of our methods provides an exact solution of the scattering equation with semi-infinite or coherent doubly semi-infinite materials. The second method is based on the treatment of a cluster embedded in a given known medium. Although less generally applicable than the exact method, it is much more efficient from a computational point of view for the treatment of surfaces. Although only pure, uncontaminated systems were studied in the present application our methods can be readily applied to substitutionally disordered alloys as well.

Both our methods were presented in terms of MT potentials but they can be readily generalized to more general cases. Also, only the treatment of coherent interfaces were considered explicitly. As mentioned in the body of the paper, the incoherent case can lead to either an extremely difficult computational task associated with supercell periodicity or to quasiperiodic behavior which would be difficult to treat conceptually as well as numerically. The treatment of arbitrary crystal structures forming an interface requires an entirely different and more general approach, which is currently being examined.

The methods presented here can be used to study a number of physically important properties of materials, including those associated with grain boundaries, interdiffusion, surface reconstruction and many others.

ACKNOWLEDGMENTS

This work was partly supported by the U.S. Department of Energy under Grant No. W-7405-ENG-48 with Lawrence Livermore National Laboratory.

-
- ¹G. F. Koster and J. C. Slater, *Phys. Rev.* **95**, 1167 (1954).
²David Kalkstein and Paul Soven, *Surf. Sci.* **26**, 85 (1970).
³E-Ni Foo and D. J. Giangiulio, *Physica B+C* **84B**, 167 (1976).
⁴J. Pollman and Sokrates T. Pantelides, *Phys. Rev. B* **18**, 5524 (1978).
⁵J. Pollman and Sokrates T. Pantelides, in *Physics of Semiconductors, 1978*, edited by B. H. Wilson (Institute of Physics, London, 1979), pp. 199–202.
⁶D. H. Lee and J. D. Joannopoulos, *Phys. Rev. B* **23**, 4988 (1981); **23**, 4997 (1981).
⁷*The Recursion Method and Its Applications*, edited by D. G. Pettifor and D. L. Weaine (Springer-Verlag, New York, 1985).
⁸R. Haydock, V. Heine, and M. J. Kelly, *J. Phys. C* **5**, 137 (1972).
⁹R. Haydock and M. J. Kelly, *Surf. Sci.* **38**, 139 (1973).
¹⁰M. C. Desjonquieres and F. Cyrot-Laukman, *J. Phys. C* **5**, 1368 (1975).
¹¹I. B. Ortenburger, S. Ciraci, and I. P. Batra, *J. Phys. C* **9**, 4185 (1976).
¹²V. Anishchik, L. M. Falicov, and F. Indurain, *Surf. Sci.* **57**, 375 (1976).
¹³E-Ni Foo, M. F. Thorpe, and D. Weaire, *Surf. Sci.* **57**, 343 (1976).
¹⁴E. J. Mele and J. D. Joannopoulos, *Phys. Rev. B* **17**, 1816 (1978).
¹⁵K. Hirabayashi, *J. Phys. Soc. Jpn.* **27**, 1475 (1969).
¹⁶K. C. Pandey and J. C. Phillips, *Solid State Commun.* **14**, 439 (1974).
¹⁷J. D. Joannopoulos and M. L. Cohen, *Phys. Rev. B* **10**, 1075 (1974).
¹⁸D. J. Chadi and M. L. Cohen, *Phys. Rev. B* **11**, 732 (1975).
¹⁹R. V. Kasowski, *Phys. Rev. Lett.* **33**, 83 (1974); *Solid State Commun.* **17**, 179 (1975).
²⁰P. G. Dempsen, L. Kleinmann, and Ed Caruthers, *Phys. Rev. B* **12**, 2932 (1975).
²¹K. S. Sohn, D. G. Dempsy, L. Kleinman, and Ed Caruthers, *Phys. Rev. B* **14**, 3185 (1976).
²²S. Ciraci and I. P. Batra, *Solid State Commun.* **18**, 1149 (1976).
²³C. Calandra and G. Santoro, *J. Vac. Sci. Technol.* **13**, 773 (1976).
²⁴C. M. Bertoni, O. Bisi, C. Calandra, and F. Manghi, *Nuovo Cimento B* **38**, 96 (1977).
²⁵D. Bisi and C. Calandra, *Nuovo Cimento B* **38**, 81 (1977).
²⁶J. D. Levine and S. G. Davison, *Phys. Rev.* **174**, 911 (1968).
²⁷S. G. Davison and J. D. Levine, *Solid State Phys.* **25**, 1 (1970).
²⁸M. Schmeits, A. Mazur, and T. Pollmann, *Phys. Rev. B* **27**, 5012 (1983).
²⁹H. L. Skriver, *The LMTO Method* (Springer Verlag, New York, 1984).
³⁰L. M. Falicov and F. Yndurain, *J. Phys. (Paris) C* **8**, 147 (1974).
³¹E. Elices and F. Yndurain, *Surf. Sci.* **29**, 540 (1972).
³²R. Riedinger and H. Dreyse, *Phys. Rev. B* **31**, 3398 (1985).
³³C. Mailhot, C. B. Duke, and D. J. Chadi, *Phys. Rev. B* **31**, 2213 (1985).
³⁴M. Schluter, J. R. Chelikowski, S. G. Louie, and Marvin L. Cohen, *Phys. Rev. B* **12**, 4200 (1975).
³⁵G. P. Koster, S. G. Louie, and Marvin L. Cohen, *Phys. Rev. B* **17**, 769 (1978).
³⁶J. R. Chelikowski, D. J. Chadi, and M. L. Cohen, *Phys. Rev. B* **23**, 4013 (1981).
³⁷J. A. Appelbaum and D. R. Hamann, *Phys. Rev. B* **6**, 2166 (1972).
³⁸J. A. Appelbaum and D. R. Hamann, *Phys. Rev. Lett.* **31**, 106 (1973).
³⁹J. A. Appelbaum, G. A. Baraff, and D. R. Hamann, *Phys. Rev. B* **11**, 3822 (1975).
⁴⁰J. A. Appelbaum, G. A. Baraff, and D. R. Hamann, *Phys. Rev. B* **14**, 1623 (1976).
⁴¹F. Garcia-Moliner and J. Rubio, *J. Phys. C* **2**, 1789 (1969).
⁴²F. Garcia-Moliner, V. Heine, and J. Rubio, *J. Phys. C* **2**, 1797 (1969).
⁴³F. Garcia-Moliner and J. Rubio, *Proc. R. Soc. London* **324**,

- 257 (1971).
- ⁴⁴F. Flores, *Nuovo Cimento B* **14**, 1 (1973).
- ⁴⁵M. Elices, F. Flores, E. Louis, and J. Rubio, *J. Phys. C* **7**, 3020 (1974).
- ⁴⁶J. A. Vergeas and E. Louis, *Solid State Commun.* **22**, 663 (1977).
- ⁴⁷J. E. Inglesfield, *J. Phys. C* **10**, 4067 (1977).
- ⁴⁸C. Noguera, D. Spanjaard, and D. W. Jepsen, *Phys. Rev. B* **17**, 607 (1978).
- ⁴⁹J. E. Inglesfield, *Surf. Sci.* **76**, 379 (1978); J. E. Inglesfield and G. Benesch, *Phys. Rev. B* **37**, 6682 (1988).
- ⁵⁰A. P. Shen and J. B. Kneger, *Phys. Rev. B* **1**, 2500 (1970); **3**, 4189 (1971).
- ⁵¹A. P. Shen, *Phys. Rev. B* **3**, 4200 (1971).
- ⁵²A. P. Shen, *Phys. Rev. B* **9**, 1328 (1974).
- ⁵³E. Wimmer, H. Krakauer, M. Weinert, and A. J. Freeman, *Phys. Rev. B* **24**, 864 (1981).
- ⁵⁴C. L. Fu, A. J. Freeman, E. Wimmer, and M. Weinert, *Phys. Rev. Lett.* **54**, 2261 (1985).
- ⁵⁵P. M. Marcus and D. W. Jepsen, *Phys. Rev. Lett.* **20**, 925 (1968).
- ⁵⁶P. J. Jennings and E. G. McRae, *Surf. Sci.* **23**, 363 (1970).
- ⁵⁷D. W. Jepsen and P. M. Marcus, in *Computational Methods in Band Theory* (Plenum, New York, 1971), p. 416.
- ⁵⁸D. W. Jepsen, P. M. Marcus, and F. Jona, *Phys. Rev. Lett.* **26**, 1365 (1971).
- ⁵⁹D. W. Jepsen, P. M. Marcus, and F. Jona, *Phys. Rev. B* **5**, 3933 (1972).
- ⁶⁰J. B. Pendry, *Low-Energy Electron Diffraction* (Academic, New York, 1974).
- ⁶¹A. Gonis, *Phys. Rev. B* **33**, 5914 (1986).
- ⁶²R. Zeller, *J. Phys. C* **20**, 2347 (1987).
- ⁶³J. Korringa, *Physica* **13**, 392 (1947).
- ⁶⁴W. Kohn and N. Rostoker, *Phys. Rev.* **94**, 1111 (1954).
- ⁶⁵P. Lloyd and P. V. Smith, *Adv. Phys.* **21**, 69 (1972).
- ⁶⁶J. S. Faulkner and G. M. Stocks, *Phys. Rev. B* **21**, 3222 (1980).
- ⁶⁷J. M. MacLaren, S. Crampin, D. D. Vvedensky, and J. B. Pendry, *Phys. Rev. B* **40**, 12164 (1989).
- ⁶⁸A. Gonis, X.-G. Zhang, and D. M. Nicholson, *Phys. Rev. B* **38**, 3564 (1988).
- ⁶⁹D. Vvedensky (private communication).
- ⁷⁰B. L. Gyorffy and M. J. Stott, in *Bank Structure Spectroscopy of Metals and Alloys*, edited by D. J. Fabian and D. M. Watson (Academic, New York, 1973), p. 385.
- ⁷¹A. R. Williams and J. van W. Morgan, *J. Phys. C* **7**, 37 (1974).
- ⁷²V. V. Babicov, *Usp. Fiz. Nauk* **93**, 3 (1967) [*Sov. Phys. Usp.* **92**, 271 (1967)].
- ⁷³F. Calogero, *Variable Phase Approach to Potential Scattering* (Academic, New York, 1967).
- ⁷⁴B. L. Gyorffy and G. M. Stocks, in *Electrons in Disordered Metals and Metallic Surfaces*, edited by P. Phariseau, B. L. Gyorffy, and L. Scheire (Plenum, New York, 1978), p. 89, and references therein.
- ⁷⁵J. S. Faulkner, in *Progress in Materials Science*, edited by J. W. Christian, P. Haasen, and T. B. Massalski (Pergamon, New York, 1982), Vol. **27**, Nos. 1 and 2, and references therein.
- ⁷⁶Kyozaburo Kambe, *Z. Naturforsch. Teil A* **22**, 322 (1967); **23**, 1280 (1968); *Surf. Sci.* **11**, 479 (1968).
- ⁷⁷M. Danos and L. C. Maximon, *J. Math. Phys.* **9**, 766 (1965).
- ⁷⁸X.-G. Zhang and A. Gonis, *Phys. Rev. Lett.* **62**, 1161 (1989).
- ⁷⁹A. Gonis, *Phys. Rev. B* **34**, 8313 (1986).
- ⁸⁰A. Gonis, G. M. Stocks, W. H. Butler, and H. Winter, *Phys. Rev. B* **29**, 555 (1984).
- ⁸¹W. H. Butler, *Phys. Rev. B* **14**, 468 (1976).
- ⁸²J. M. MacLaren, X.-G. Zhang, A. Gonis, and S. Crampin, *Phys. Rev. B* **40**, 9955 (1989).
- ⁸³M. E. McHenry, J. M. MacLaren, M. E. Eberhart, and S. Crampin, *J. Magn. Magn. Mater.* (to be published).

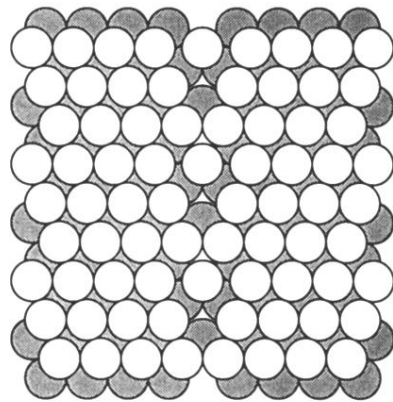


FIG. 9. Atomic structure at a Σ_3 tilt grain boundary in Fe.